

Chapter 9:

Tables and Figures

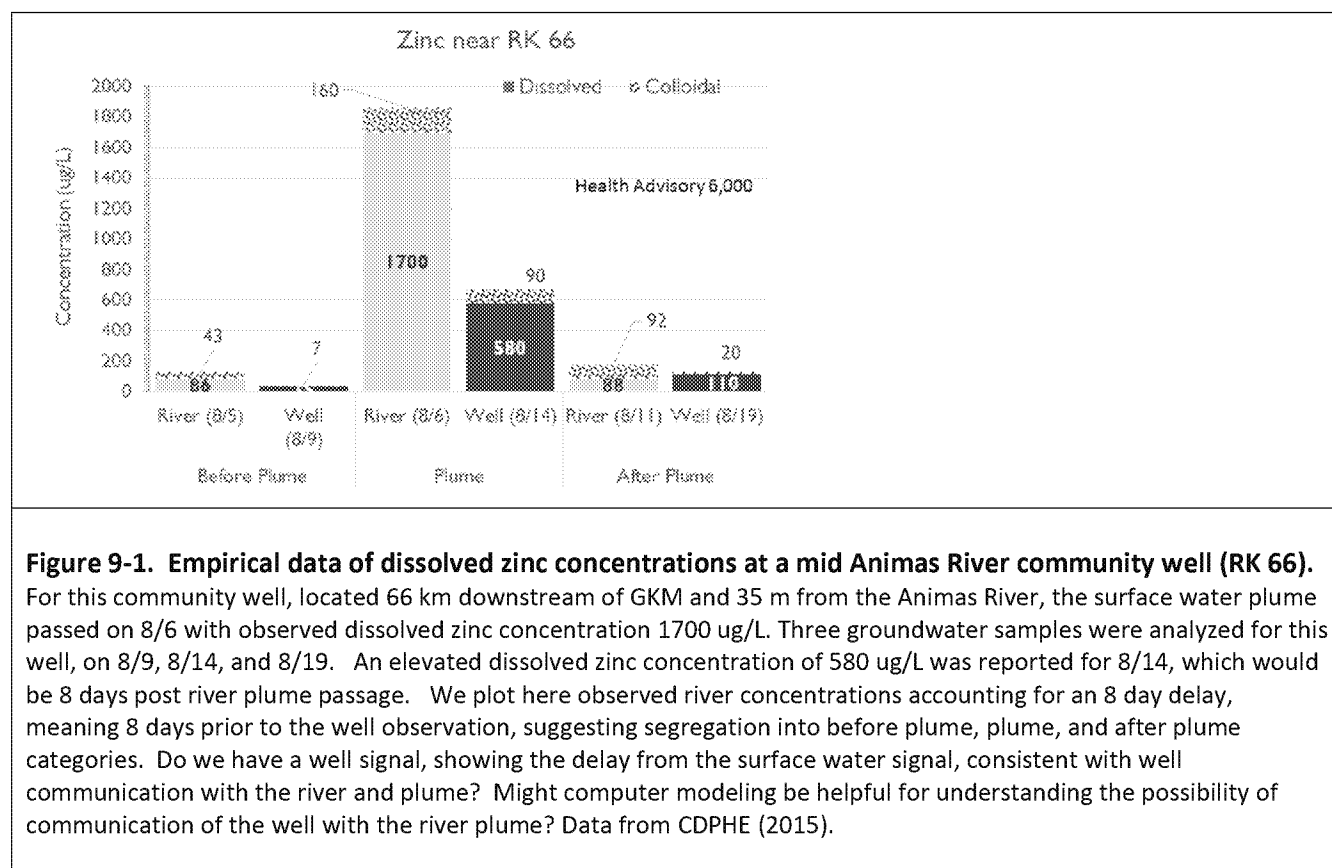
List of Tables

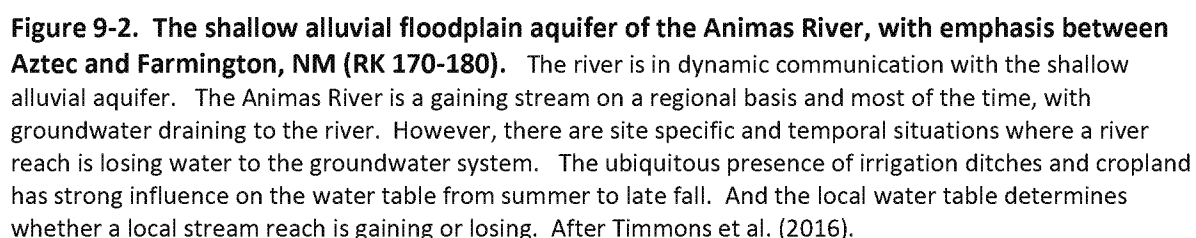
Table 9-1. Conceptual Complexity and Groundwater Model Selection	12
--	----

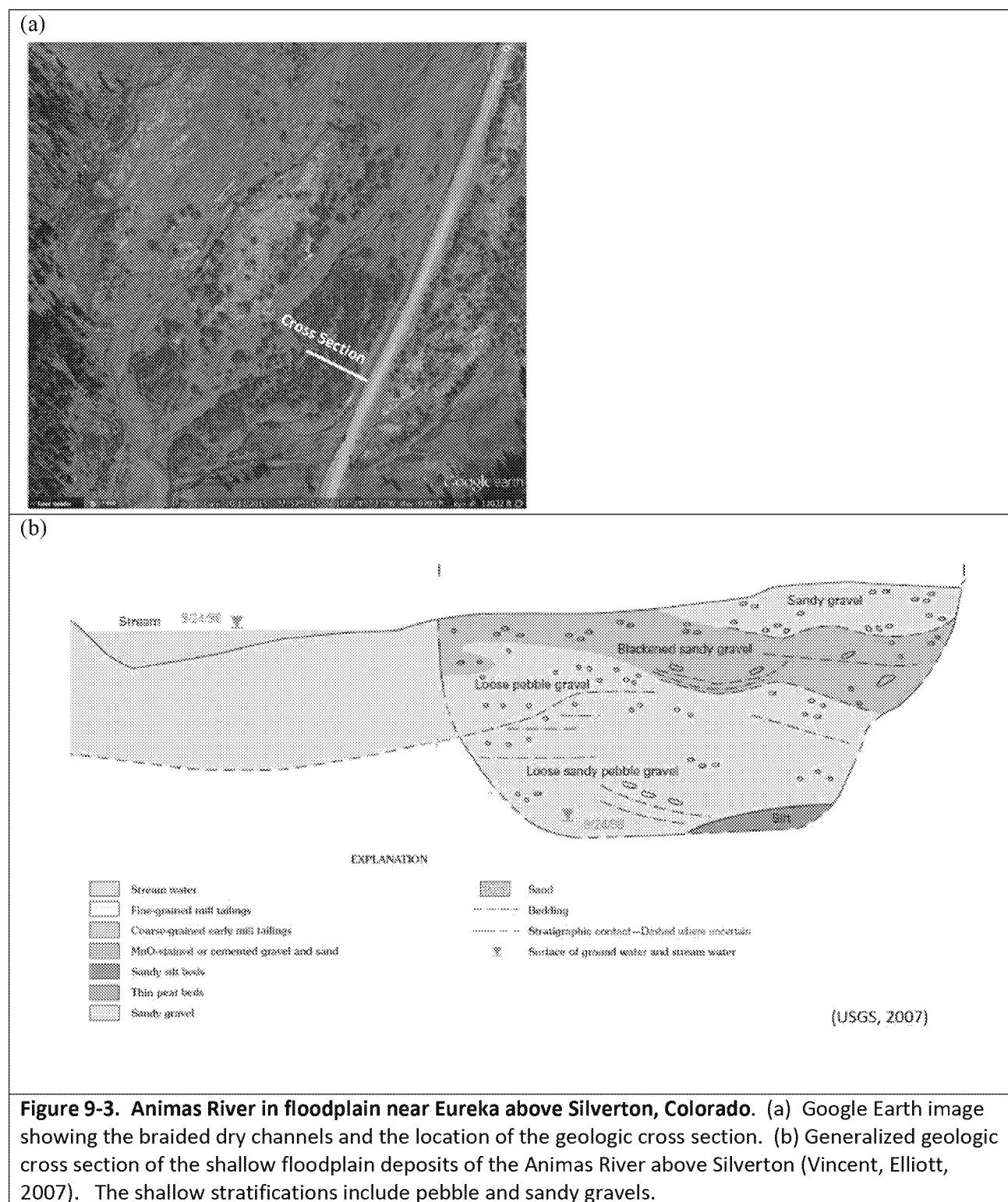
List of Figures

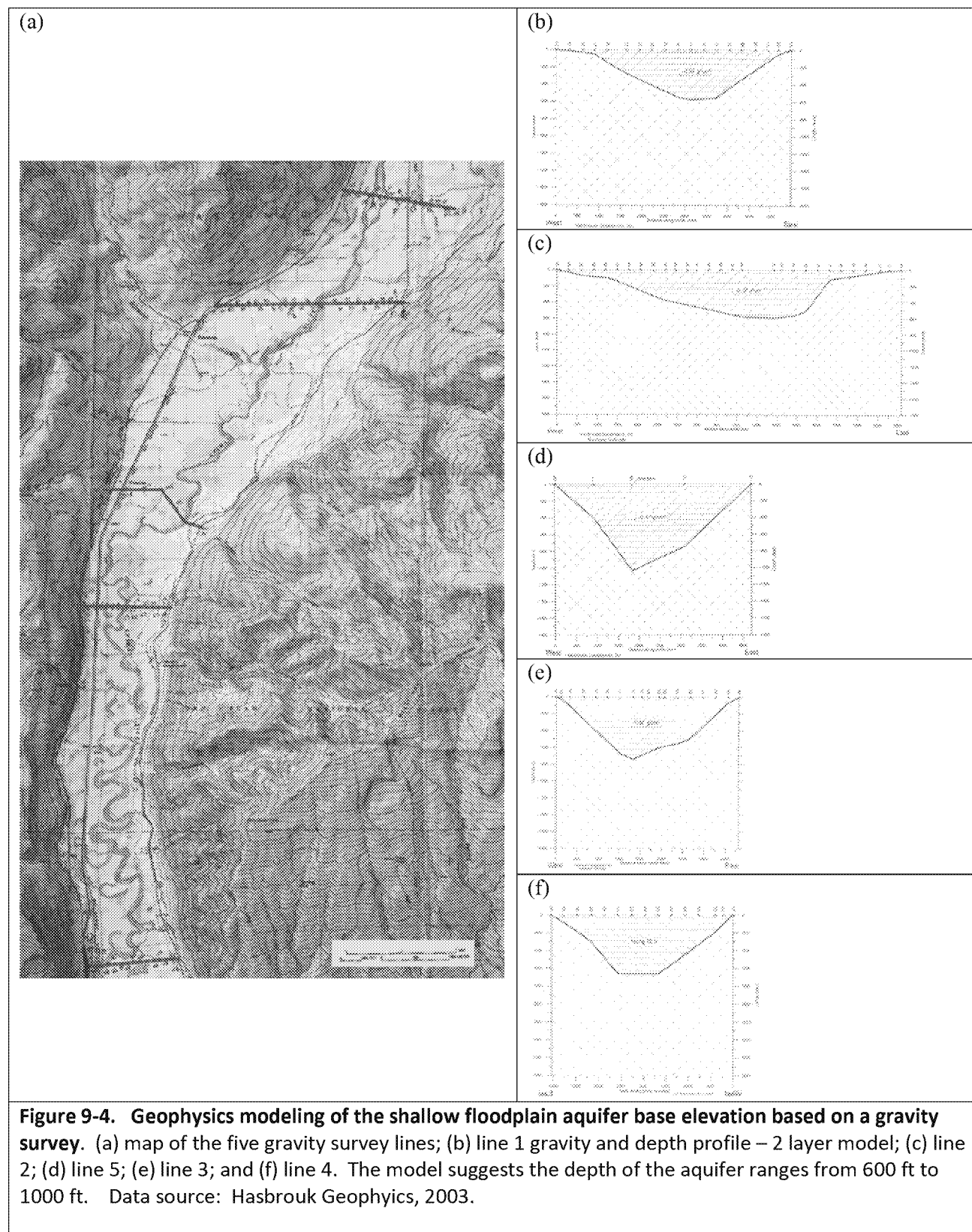
Figure 9-1. Empirical data of dissolved zinc concentrations at a mid Animas River community well (RK 66).	4
Figure 9-2. The shallow alluvial floodplain aquifer of the Animas River, with emphasis between Aztec and Farmington, NM (RK 170-180)..	5
Figure 9-3. Animas River in floodplain near Eureka above Silverton, Colorado.	6
Figure 9-4. Geophysics modeling of the shallow floodplain aquifer base elevation based on a gravity survey.....	7
Figure 9-5. Demonstration of a pumping well capture zone and particle tracking breakthrough histogram using the WhAEM groundwater model of a hypothetical scenario..	8
Figure 9-6. The mid Animas and lower Animas River clusters of community and private wells selected for groundwater modeling analyses..	9
Figure 9-7. Water supply wells of the floodplain of the mid Animas River.	10
Figure 9-8. Streamflow analysis of the upper Animas River near Silverton, Colorado.....	11
Figure 9-9. GFLOW layout of analytic elements for the mid Animas River floodplain groundwater model.	13
Figure 9-10. GFLOW model of the mid Animas River floodplain near Baker's Bridge (RK 65-72) showing groundwater-surface water interactions for the averaging period August-October 2015..	14
Figure 9-11. GFLOW capture zone and solute breakthrough histogram for a mid Animas River community well..	15
Figure 9-12. Community wells (orange) and select private wells (red) for the Lower Animas River floodplain study area.	16
Figure 9-13. High resolution synoptic survey of the river water levels and well water levels in the lower Animas River floodplain, January 2016, between Riverside and Farmington, New Mexico..	17
Figure 9-14. Hydrographs from Aztec area including a well with continuous data recorder plotted with influences from precipitation and Animas River stage and ditch gage height.	18
Figure 9-15. GFLOW model of groundwater-surface water interactions in the lower Animas River floodplain between Aztec and Farmington, New Mexico (RK 170-180) for the averaging period August – October 2015.	19

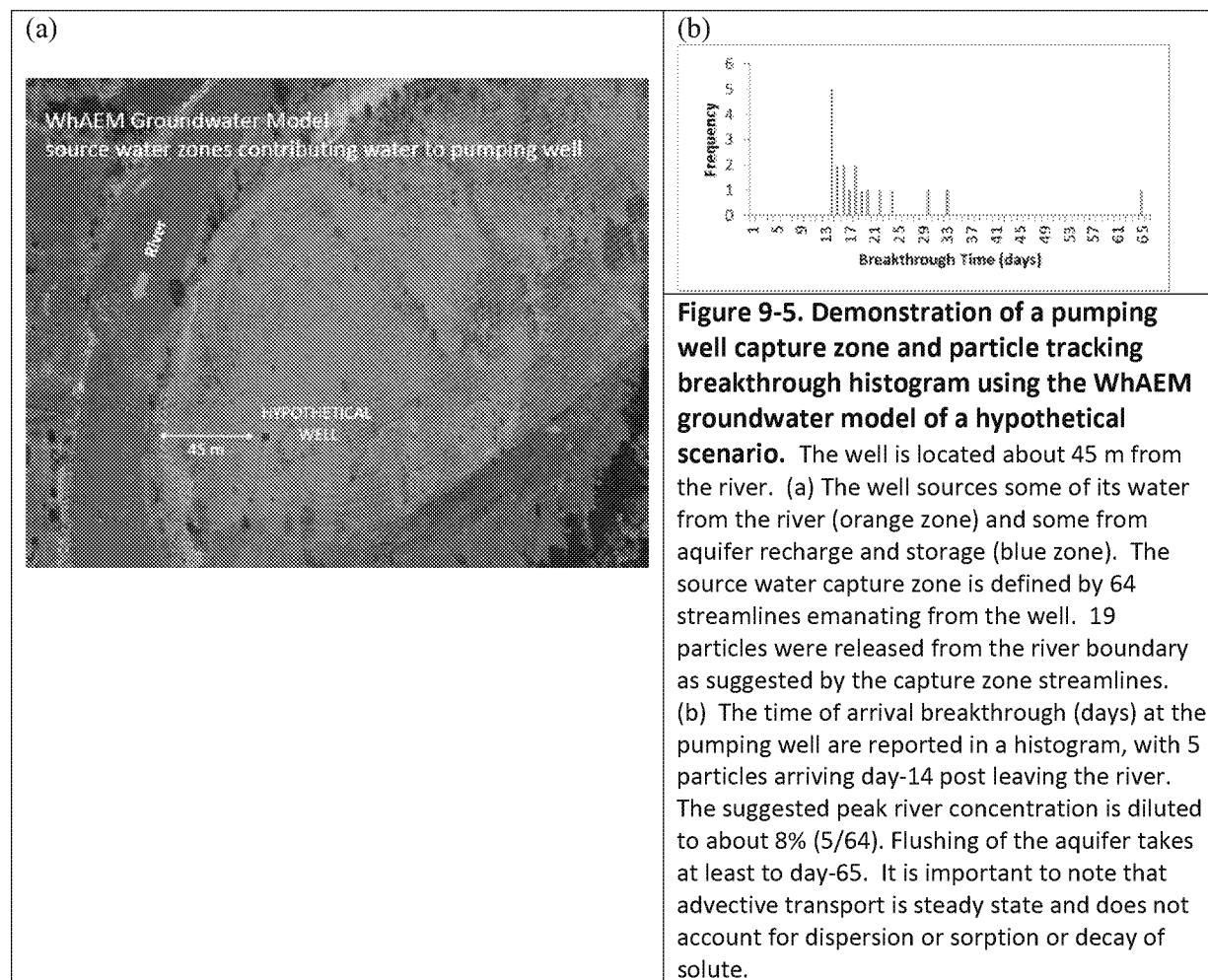
Figure 9-16. GFLOW capture zone and solute breakthrough histogram for lower Animas community well. GFLOW analysis of Lower Animas River community well (21m-174km), high pumping ($Q_w=817.6$ m ³ /d) and low porosity ($n=0.25$).	20
Figure 9-17. River and well dissolved and colloidal metals concentrations around RK 66 of the mid Animas River in Colorado..	21
Figure 9-18. River and well dissolved and colloidal metals concentrations around RK 163 of the lower Animas River in New Mexico.	22

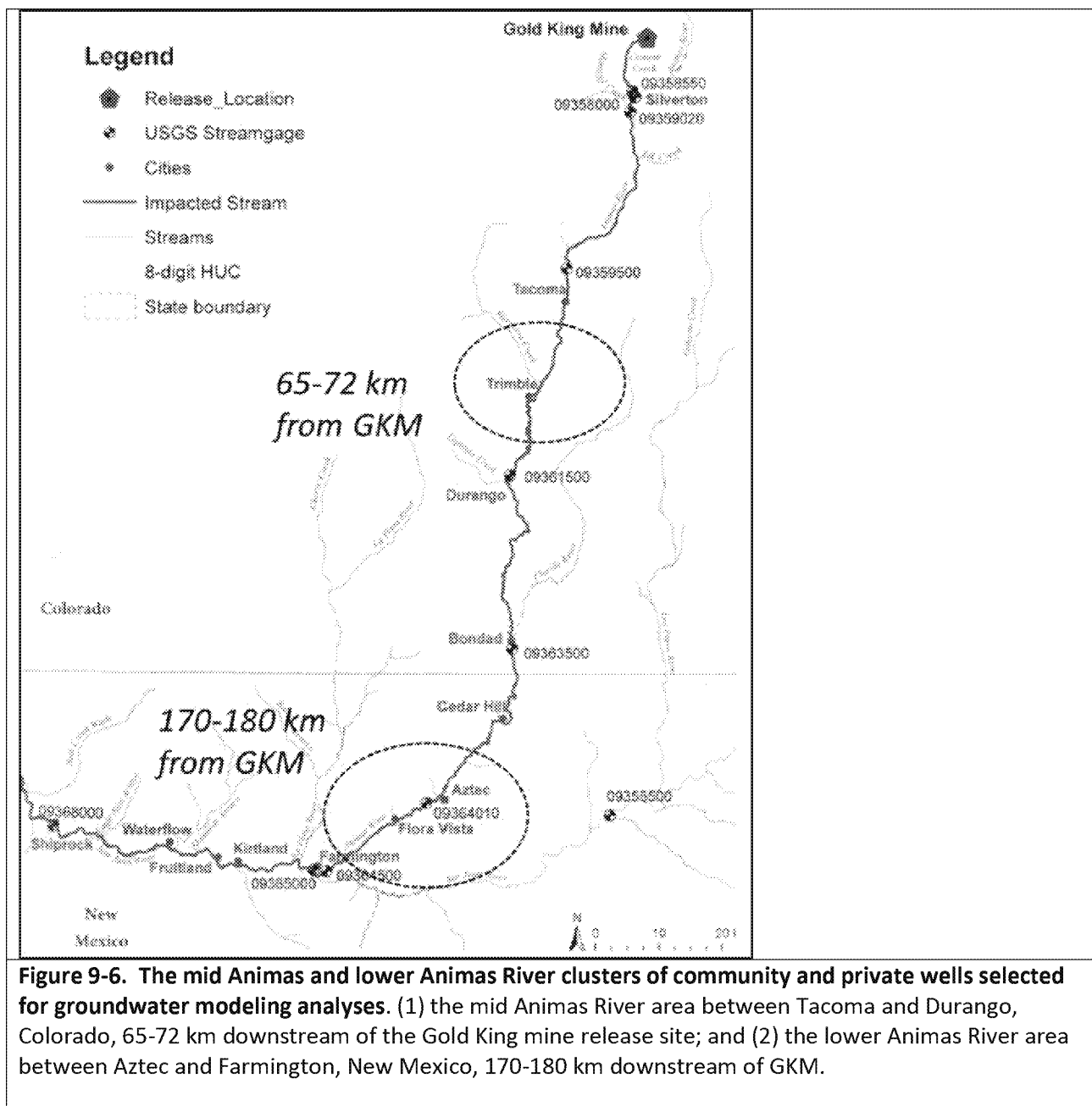


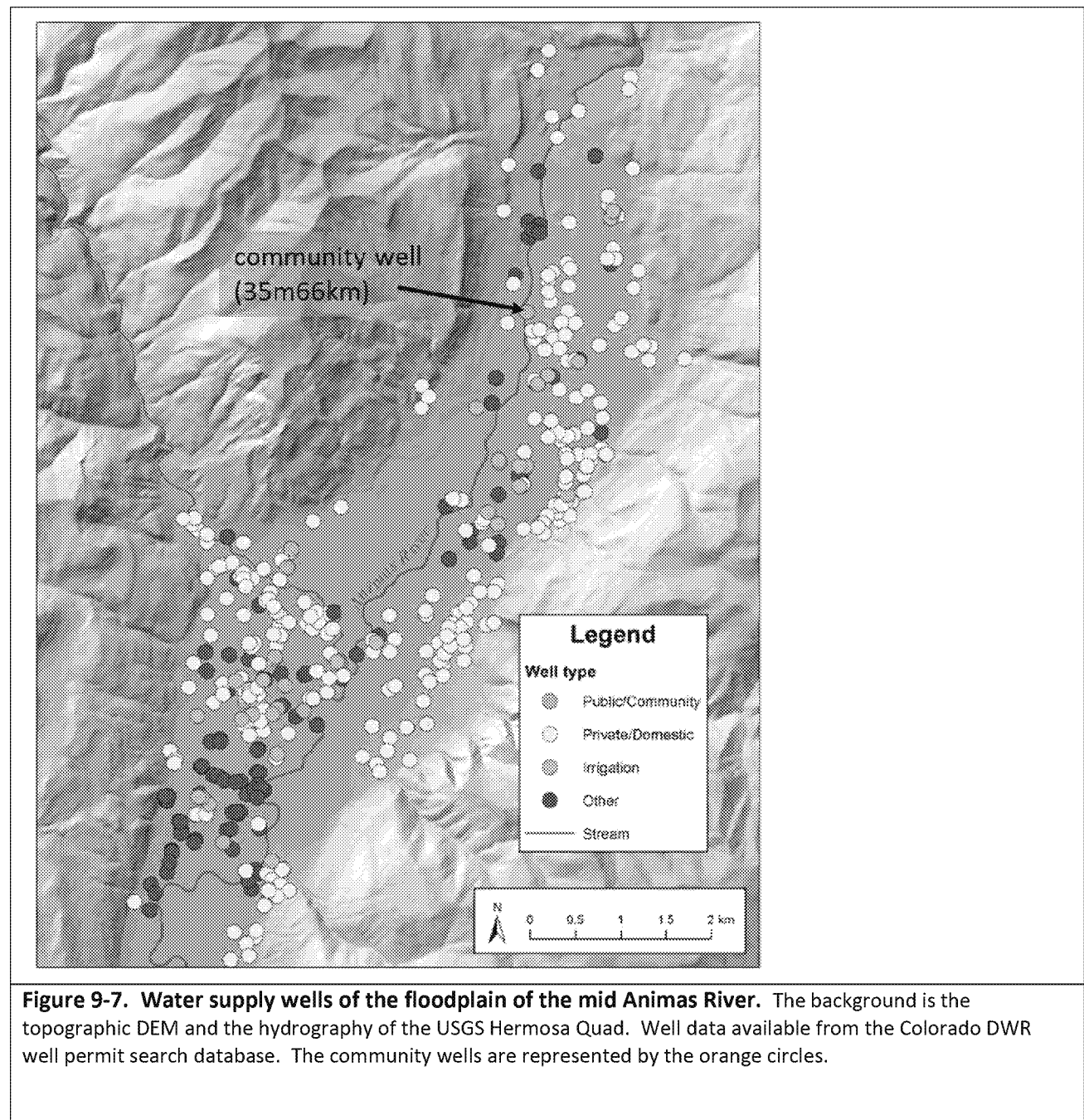












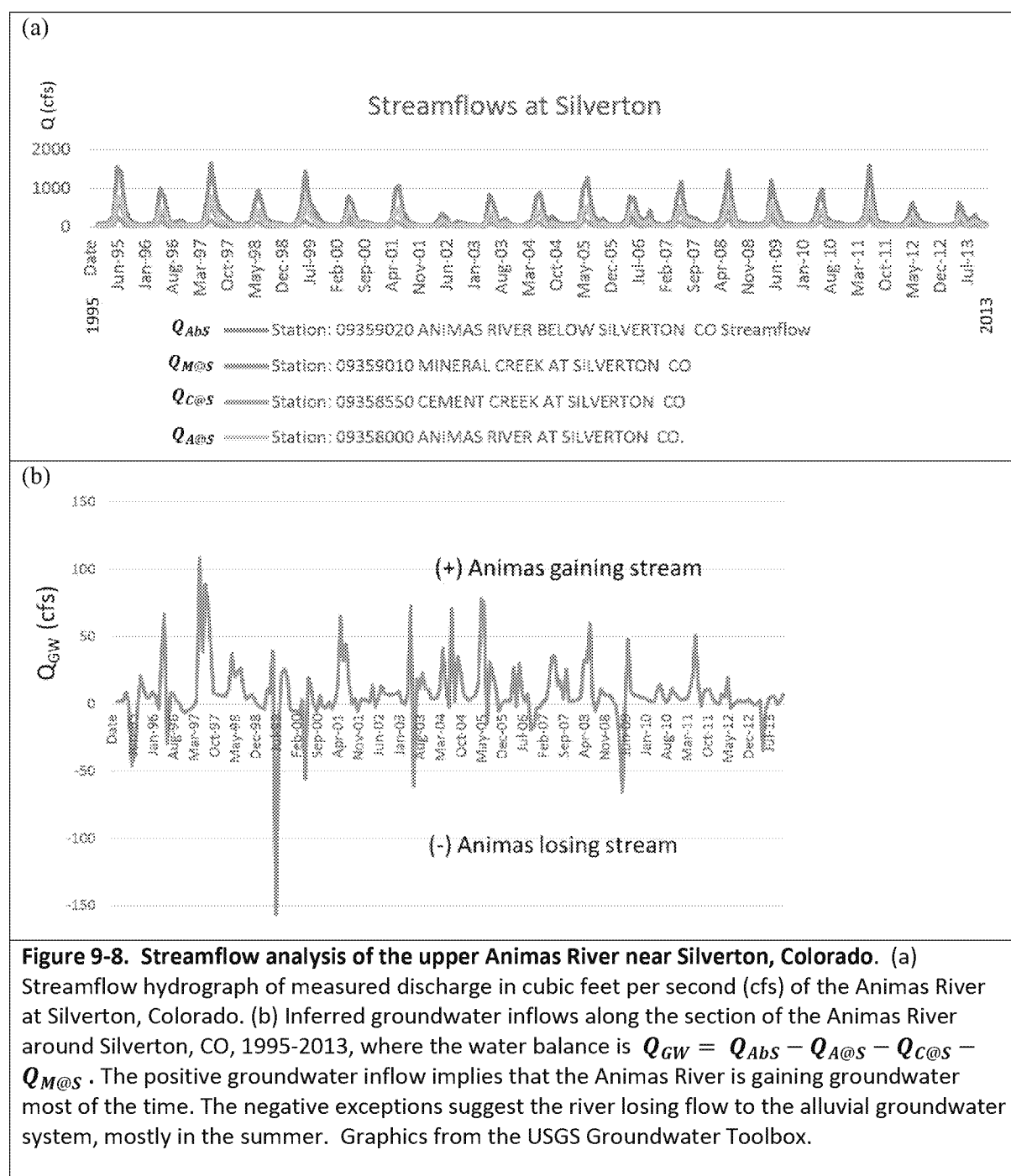
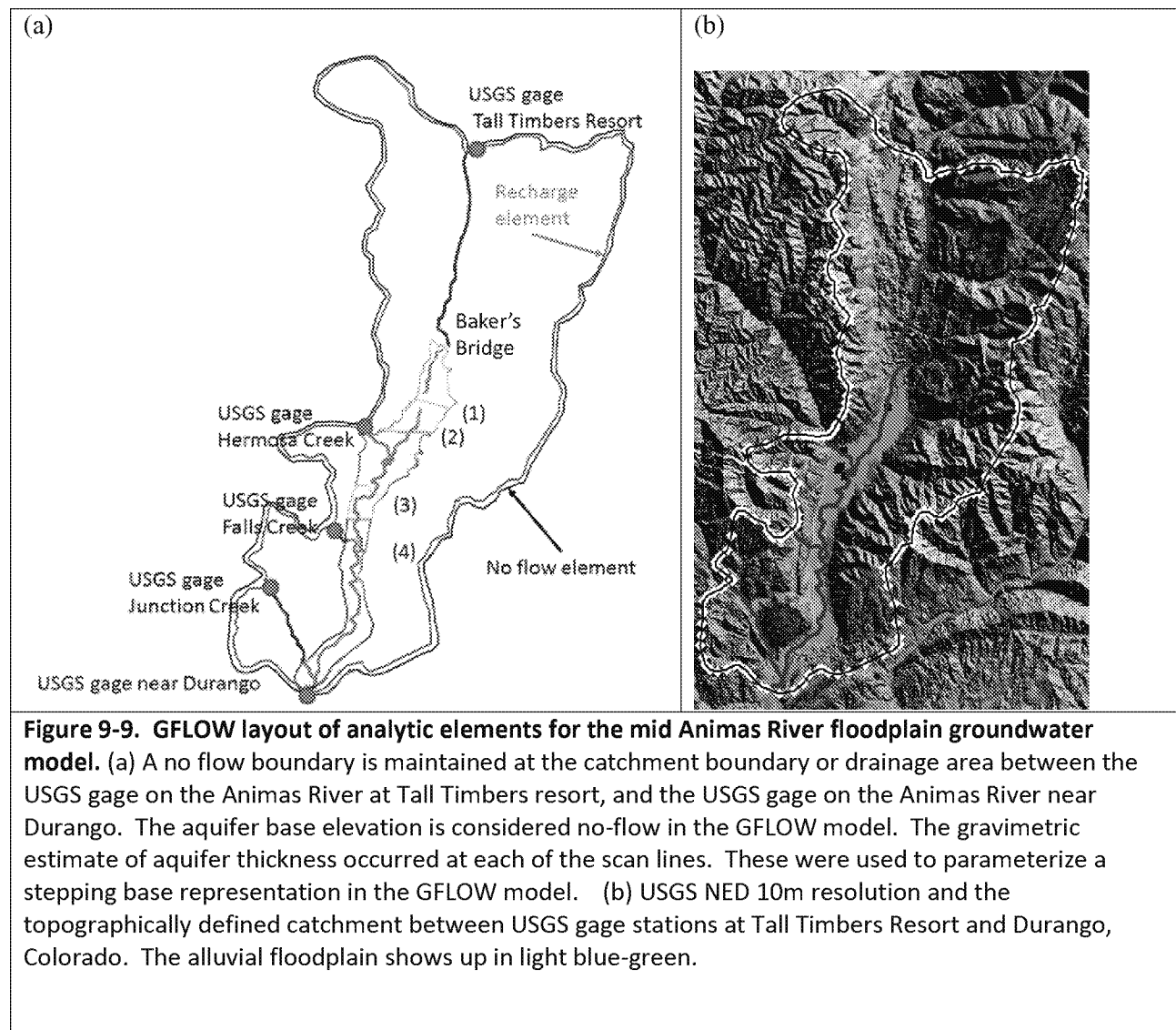


Table 9-1. Conceptual Complexity and Groundwater Model Selection

	Conceptual Complexity	GFLOW	MODFLOW
1.	Single Layer aquifer (piecewise homogeneous properties, horizontal base elevations, point sinks for wells, line-sinks for rivers, area elements for zoned recharge and aquifer properties)	<input checked="" type="checkbox"/>	
2.	Dupuit Forchheimer assumption (neglect resistance to vertical flow; hydraulic heads constant with depth, horizontal 2D flow)	<input checked="" type="checkbox"/>	
3.	Non-time variant (steady state) stress and flow	<input checked="" type="checkbox"/>	
4.	Time-variant (transient) stress and flow		<input checked="" type="checkbox"/>
5.	Three dimensional flow		<input checked="" type="checkbox"/>
6.	Particle tracking (reverse – capture zones; forward – breakthrough response)	<input checked="" type="checkbox"/>	<input checked="" type="checkbox"/>



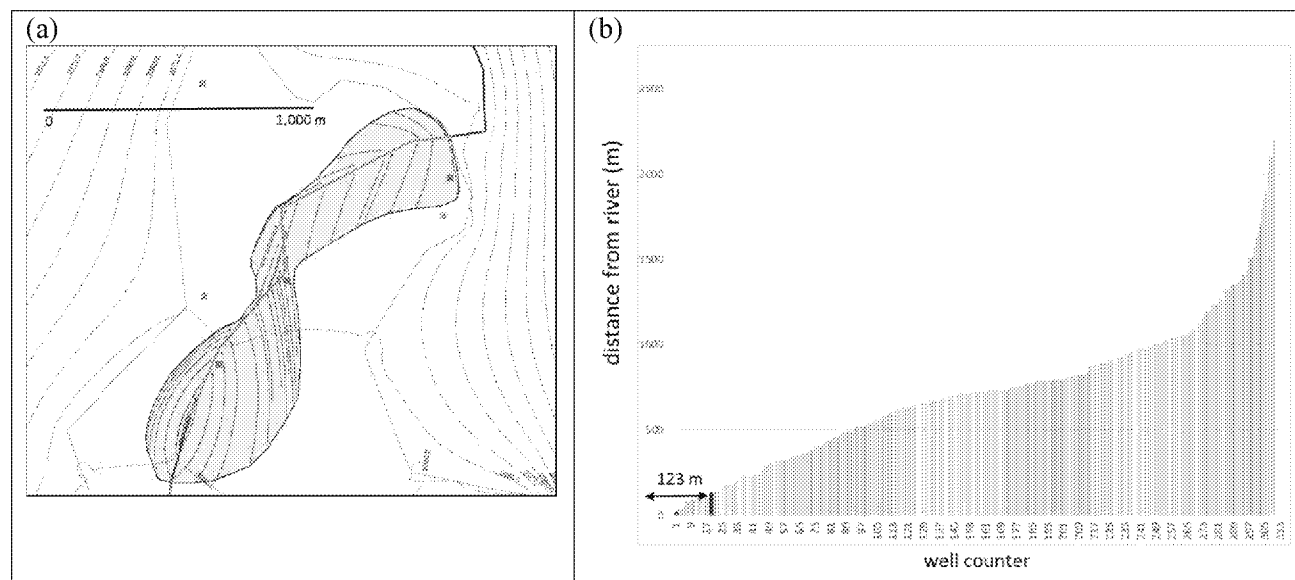


Figure 9-10. GFLOW model of the mid Animas River floodplain near Baker's Bridge (RK 65-72) showing groundwater-surface water interactions for the averaging period August-October 2015. (a) Hydraulic head contours (m) are shown as dotted lines and the river flow is north to south. Model calibration is discussed in Appendix D. The gaining sections of the river are colored black; the losing sections shown in green. Forward particle traces are shown in red, with residence time limited to 90 days time-of-travel. Note there are three private domestic pumping wells located inside the "hyporheic" zone colored light red. (b) The bar graph shows the distances of wells from the river of over 300 wells. Distances ranged from 10m to over 2000 m. The GFLOW model found that only three wells (including 5 community wells) in the mid Animas River area, and distances of the wells from the river ranged from 10-123 m. There were many other wells within 123 m of the river that the model suggested do not source river water. Therefore distance from the river alone is not predictive of well sourcing from the river. Geomorphology and the location of losing sections of the river are factors. The model suggests that the Baker's Bridge area where the Animas River leaves the mountain pass and enters the floodplain valley has groundwater seeping into the aquifer.

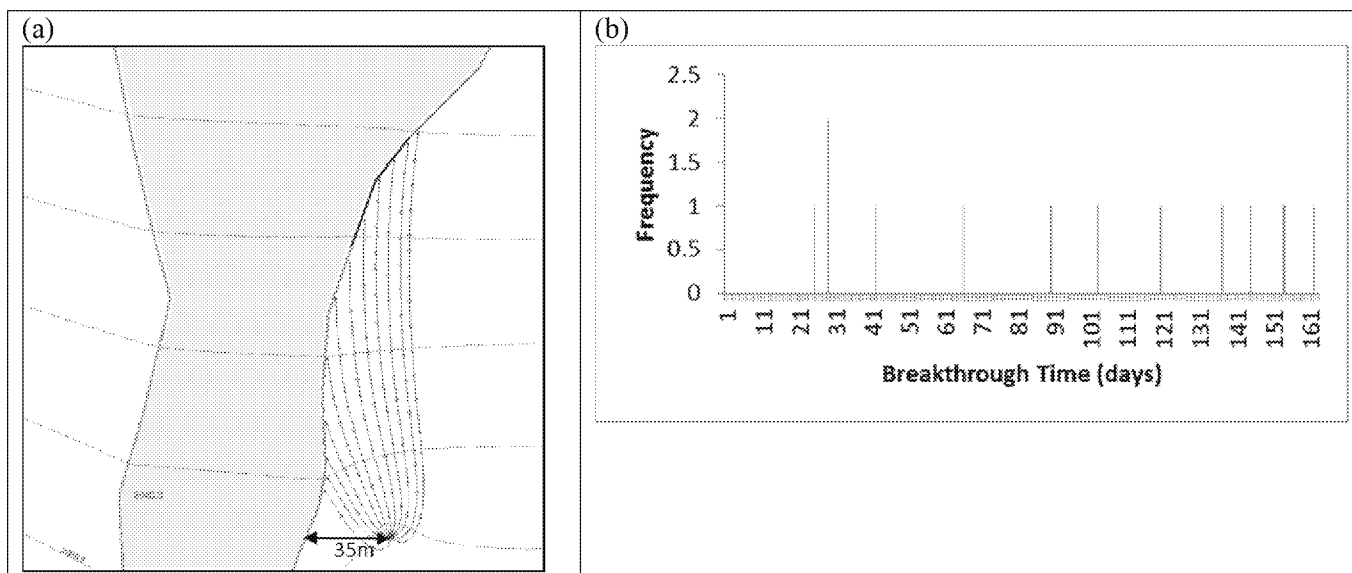
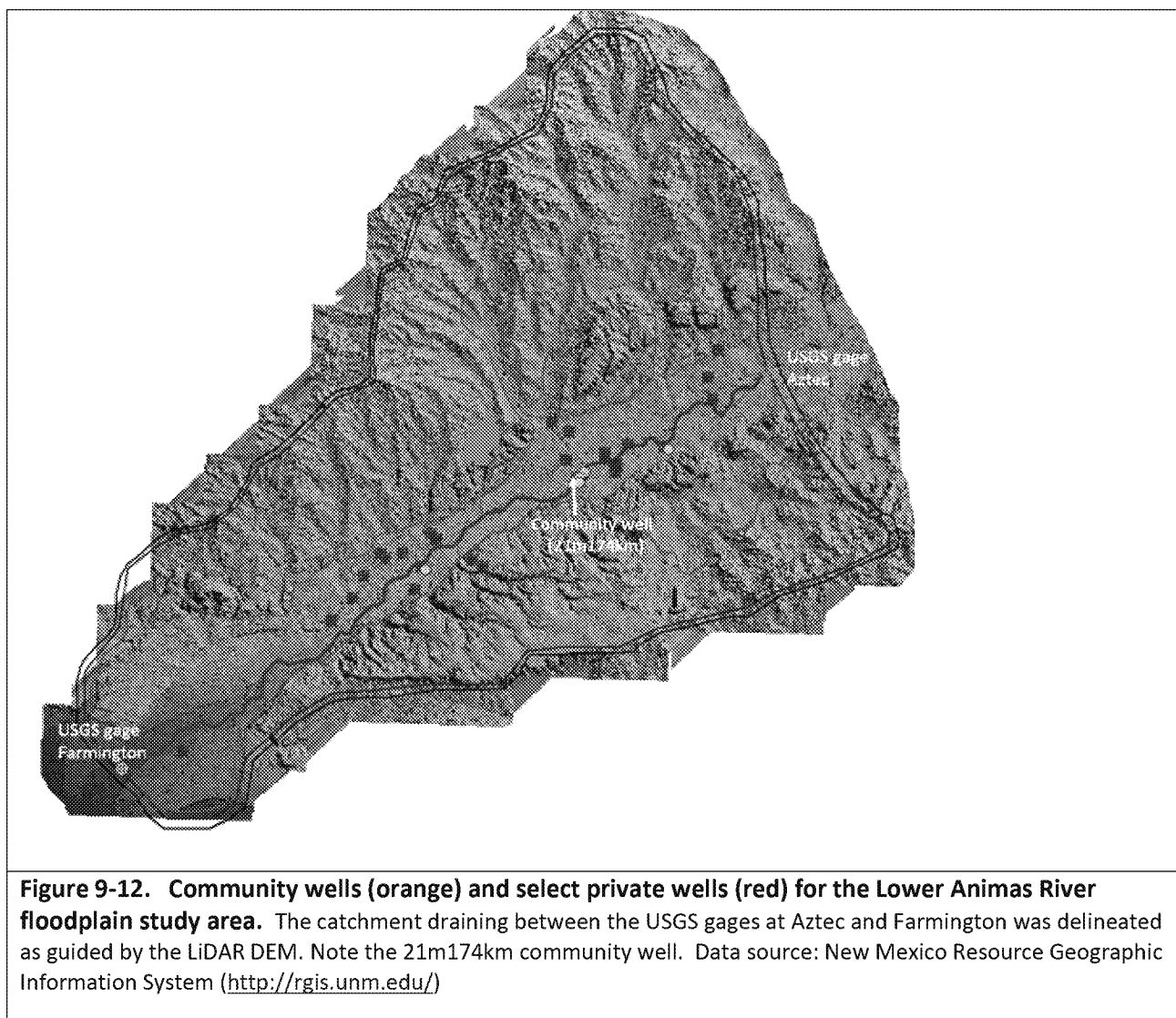


Figure 9-11. GFLOW capture zone and solute breakthrough histogram for a mid Animas River community well. GFLOW analysis of mid Animas River community well (35m-66km), high pumping ($Q_w = 2,616.5 \text{ m}^3/\text{d}$) and low porosity ($n=0.2$) (a) particle tracking with 12 forward pathlines; (b) time of arrival breakthrough (days) are reported in a histogram, with a particle arriving in 25 days. Breakthrough time with same pumping but higher porosity ($n=0.35$) has a particle arriving in 44 days. Suggested peak river concentration is diluted to about 17% ($2/12$). Flushing of the aquifer in about 160 days. Full sensitivity analysis on area recharge, hydraulic conductivity of aquifer material, and pumping rate of well is described in Appendix D. Note that advective transport is steady (time invariant pumping and hydrology) and does not account for dispersion, sorption, or decay of solute.



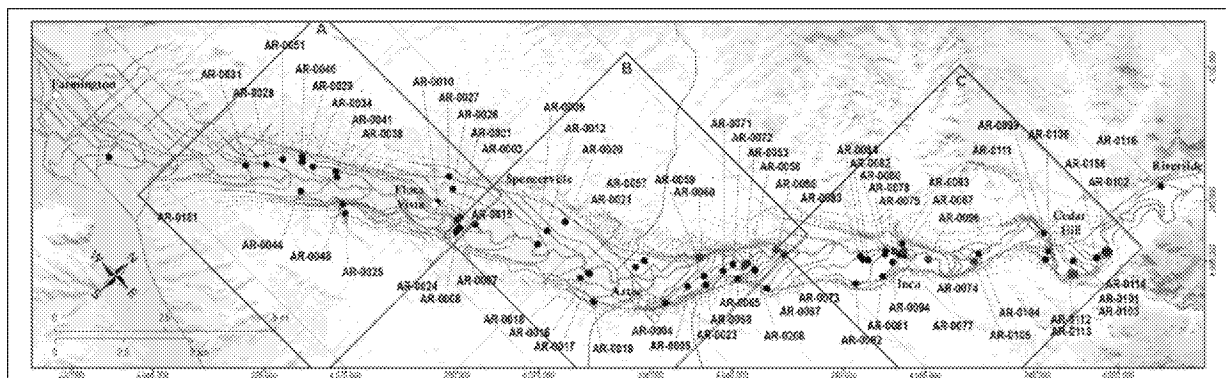
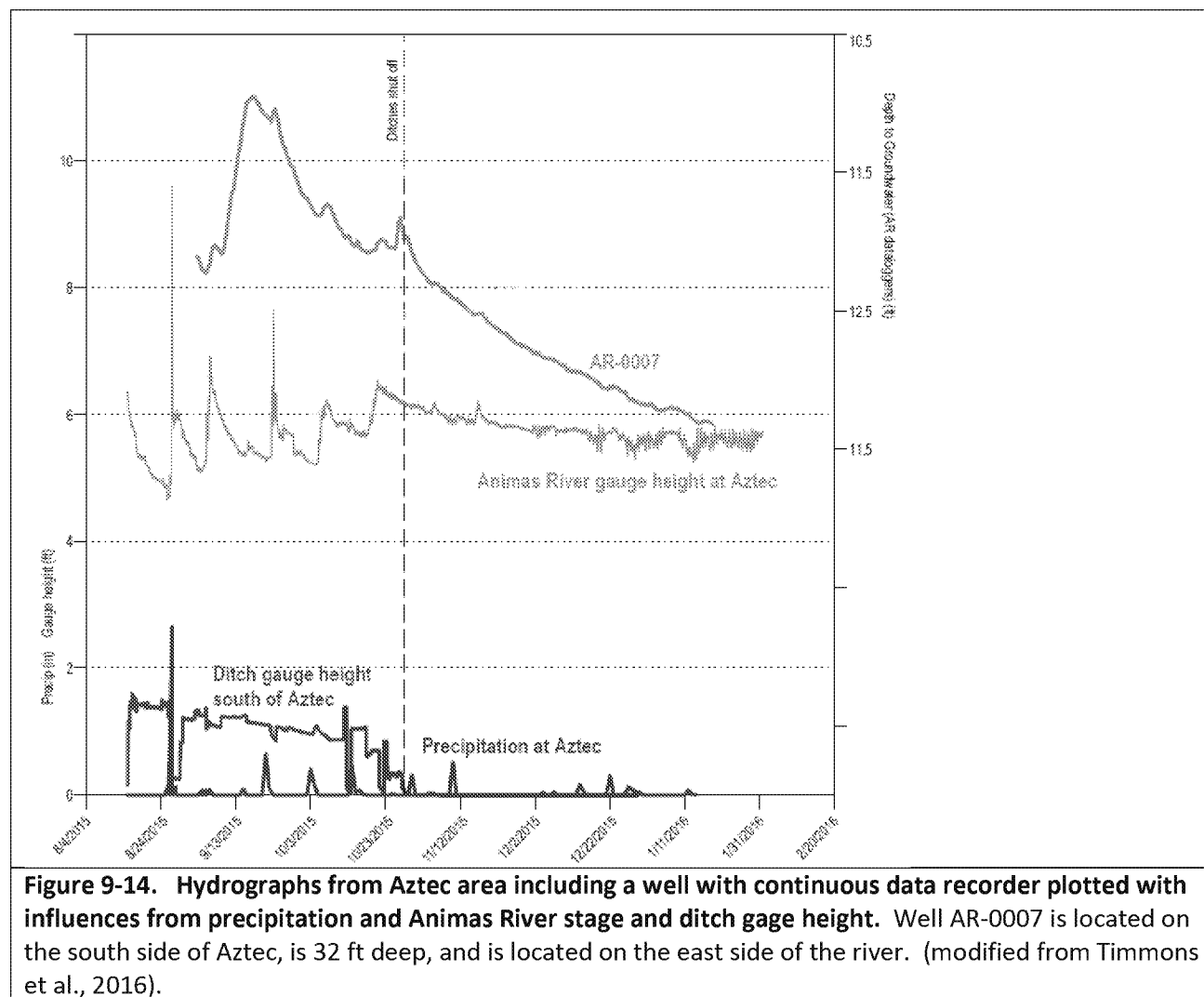


Figure 9-13. High resolution synoptic survey of the river water levels and well water levels in the lower Animas River floodplain, January 2016, between Riverside and Farmington, New Mexico. The wells were geospatially located using hand-held GPS. A high resolution LiDAR DEM was used to estimate land surface elevations. Data collection supports the New Mexico Bureau of Geology and Mineral Resources Aquifer Mapping Program (Timmons et al, 2016). The wells with negative gradient (shown as red dots) indicated segments of the Animas River that were losing river water to the aquifer.



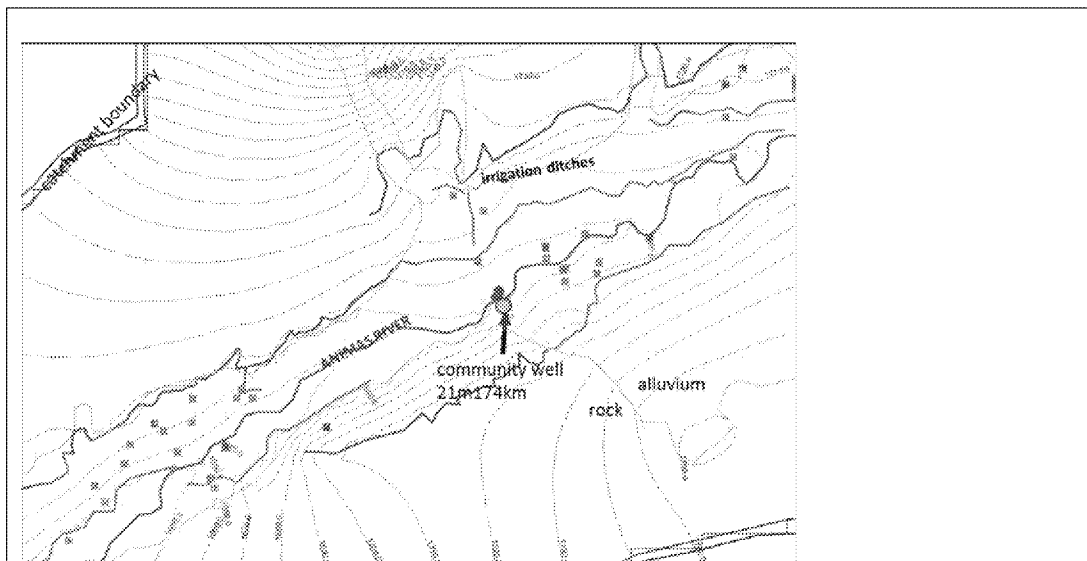
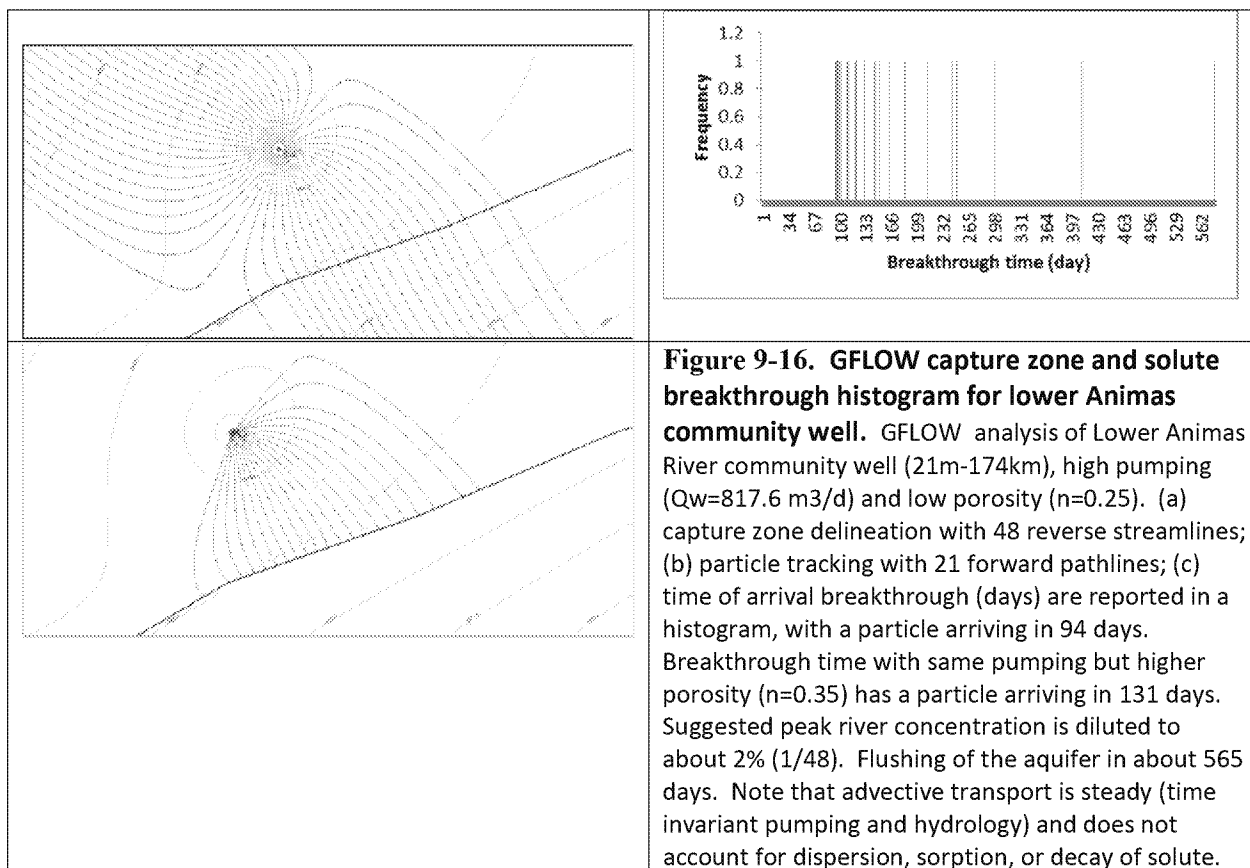


Figure 9-15. GFLOW model of groundwater-surface water interactions in the lower Animas River floodplain between Aztec and Farmington, New Mexico (RK 170-180) for the averaging period August – October 2015. Model calibration is described in Appendix D. Effective areal recharge is $0.21\text{E-}4$ m/d. Rock hydraulic conductivity is 0.035 m/d and alluvium hydraulic conductivity is 2.2 m/d. The river and irrigation ditches are represented as line-sinks. The private and community wells are represented as point sinks. The 90 day capture zones of the wells are too small to be seen at this scale. The model suggests only the 21m-174km community well pumping at a maximum rate of 817.6 m³/d sources from the river.



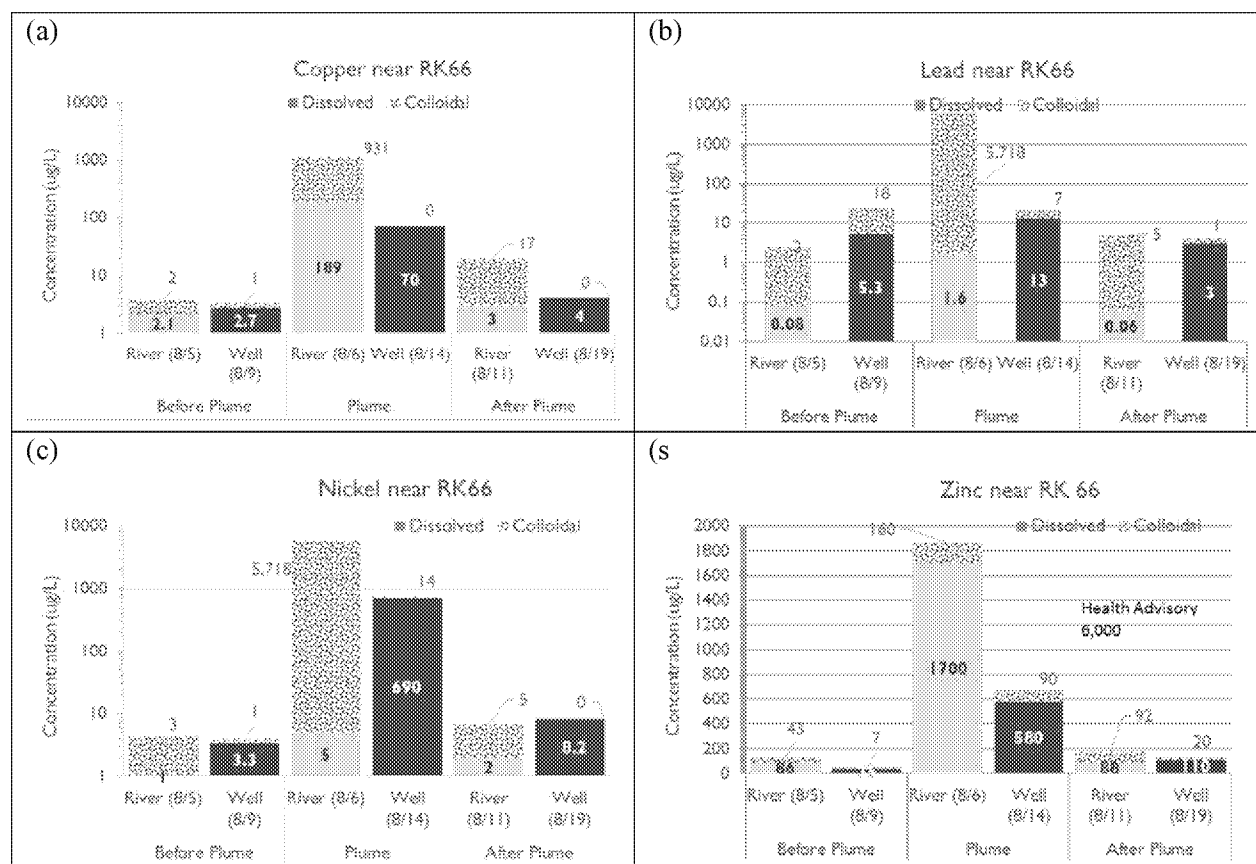


Figure 9-17. River and well dissolved and colloidal metals concentrations around RK 66 of the mid Animas River in Colorado. The data is organized into before, during, and after plume time windows assuming the peak river plume passed the location on 8/6 and a potential 8 day lag in transport in the groundwater system before arrival at the well.

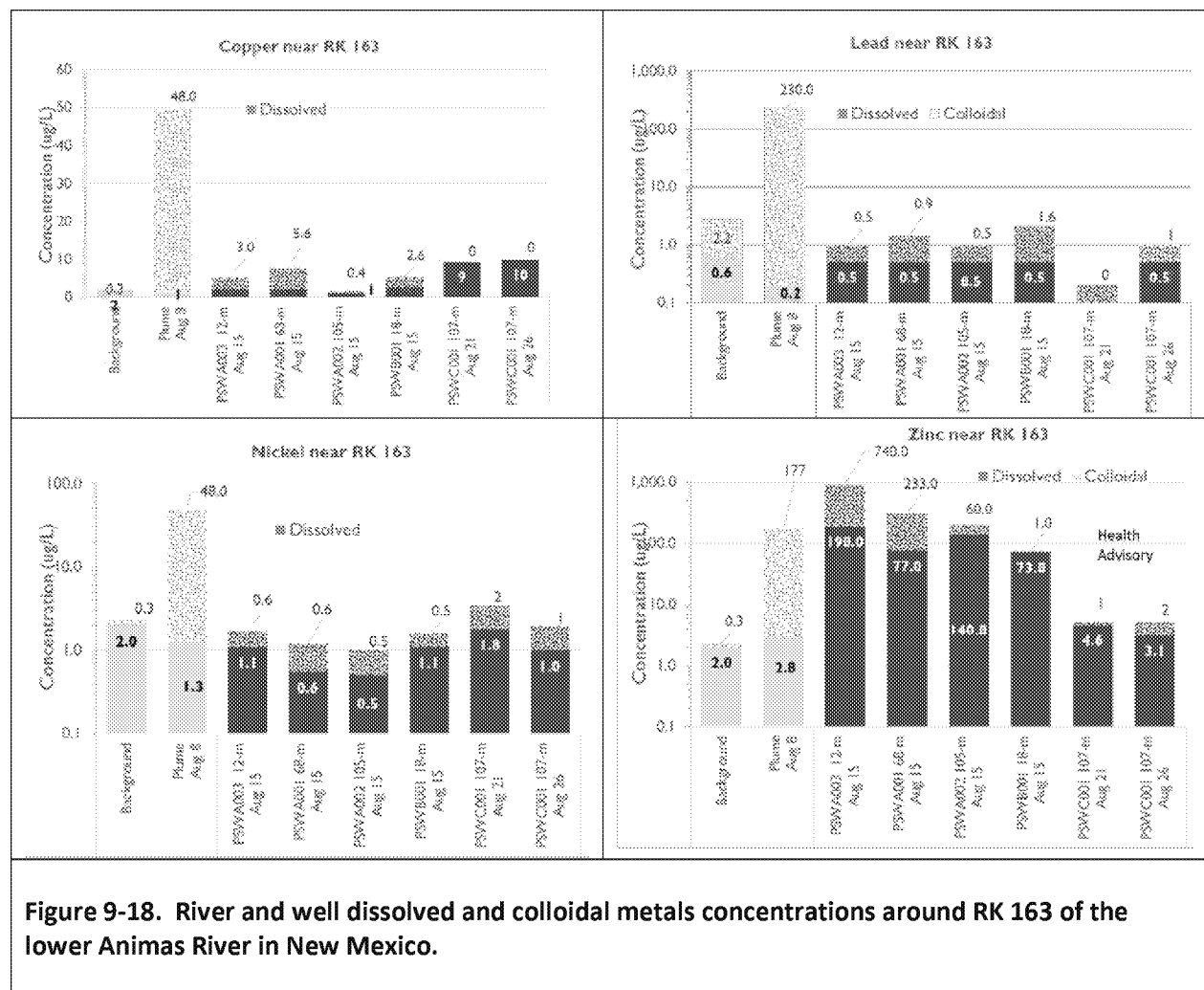


Figure 9-18. River and well dissolved and colloidal metals concentrations around RK 163 of the lower Animas River in New Mexico.

